

Anomalous values of interaction constants in the two-dimensional electron gas of a silicon metal-oxide-semiconductor field-effect transistor measured by parallel- and perpendicular-field magnetoconductivity

M. S. Burdis and C. C. Dean

Department of Physics, University of Exeter, Stocker Road, Exeter EX4 4QL, England

(Received 19 November 1987; revised manuscript received 9 March 1988)

Comprehensive measurements of magnetic-field and temperature dependence of electrical conductivity in the two-dimensional electron gas of a silicon metal-oxide-semiconductor field-effect transistor reveal unexpected values of interaction constants. Parallel-magnetic-field measurements show previously unseen dependencies on both temperature and carrier concentration, and these observations are corroborated by analysis of the temperature dependence of conductivity in both zero and small perpendicular magnetic fields.

I. INTRODUCTION

The magnetic-field and temperature dependence of the electrical conductivity (σ) of a disordered electronic system can yield much useful information about its microscopic properties. In this paper we initially review the currently accepted transport theories of weakly disordered systems, with particular reference to the two-dimensional electron gas (2D EG) formed at the Si/SiO₂ interface in a metal-oxide-semiconductor field-effect transistor (MOSFET). We then describe our experimental techniques and measurements. Finally, we discuss the significance of our findings and offer a possible explanation for these observations.

Our measurements can be divided into four separate areas.

(1) Parallel-field magnetoconductivity [$\sigma(B_{\parallel})$] which we find is anomalously large.

(2) Temperature dependence of conductivity [$\sigma(T)$] with no applied magnetic field, which gives information relating to both interaction and localization effects.

(3) Low-perpendicular-field magnetoconductivity [$\sigma(B_{\perp})$] which shows the characteristic parameters of localization, permitting untangling of the interaction constant from the temperature-dependence measurement.

(4) Temperature dependence of conductivity [$\sigma(T, B_0)$] with a small perpendicular magnetic field applied. The magnetic field should suppress weak localization effects, and thus provide a third independent measurement of the interaction constants.

Previous experimentalists (Bishop, Dynes, and Tsui,¹ in particular) have reported measurements showing unexpectedly high values of interaction constants obtained by parallel-field magnetoconductivity experiments. We confirm these observations, and find further discrepancies in the theory regarding temperature dependence of the interaction constants.

The MOSFET provides an ideal system to study electronic processes in two dimensions. This is due to a very

thin (approximately 10 nm) electron inversion layer at the semiconductor-insulator interface. In addition, by changing the voltage applied to the gate, the number of carriers in the inversion layer can be controlled easily and precisely. This allows a wide range of measurements to be made on a single device. (See the review by Ando, Fowler, and Stern.²)

The conductivity of an inversion layer in a silicon MOSFET is affected profoundly by localization phenomena and electron-electron interactions. According to the scaling theory of localization^{3,4} a two-dimensional system is said to be weakly localized in the presence of small but finite amounts of disorder. This has the effect of reducing the conductivity at very low temperatures from the Boltzmann or Drude value. The weak-localization theory is only valid in the regime where the distance an electron travels before being scattered is greater than its Fermi wavelength, i.e., $k_F l > 1$, where l is the elastic mean free path, and k_F the Fermi wave vector.

The effect of electron-electron interaction in the presence of disorder is to reduce the density of states at or close to the Fermi level.⁵⁻⁷ This again has the effect of reducing the conductivity from the semiclassical value.

In an independent-electron model, weak-localization considerations predict a logarithmic temperature dependence to the conductivity in 2D. On the other hand, when considering only interaction effects, a similar logarithmic correction is predicted. The two phenomena are consequently very difficult to distinguish by measuring $\sigma(T)$.

In a perpendicular-magnetic-field measurement the negative electron-electron interaction magnetoconductivity can be masked by the positive localization effect. Further complications can arise from Landau-level effects, which cause the conductivity to oscillate. It is, consequently, very difficult to obtain useful information regarding interaction processes from perpendicular magnetic-field measurements.

If, however, the sample is aligned exactly parallel to the magnetic field, the localization and orbital effects will be absent and the interaction effects, which are largely independent of field orientation, can be measured.

II. THEORETICAL BACKGROUND

Theoretical work has concentrated on two main areas: first, localization of noninteracting electrons due to disorder in the system which reduces the diffusivity of the electrons, and, second, electron-electron interactions in the presence of disorder which lead to a correction to the single-particle density of states. If we write the conductivity σ as

$$\sigma = e^2 N(E_F) D(E_F), \quad (1)$$

where $D(E_F)$ is the diffusion coefficient and $N(E_F)$ is the density of states at the Fermi energy E_F , it can easily be seen that first-order corrections to either $D(E_F)$ or $N(E_F)$ will produce first-order changes in the conductivity. Both $D(E_F)$ and $N(E_F)$ show temperature dependence and so both of the effects described will lead to a temperature dependence of conductivity. In two dimensions, theories based on localization and interaction predict rather similar behavior for the conductivity as a function of temperature [i.e., σ has $\ln(T)$ dependence], and so the two mechanisms are difficult to distinguish.

Following the work of Thouless³ and Abrahams *et al.*,⁴ the scaling-length dependence of the conductivity of a 2D EG is given by

$$\sigma(L) = \sigma(L_0) - \frac{\alpha e^2}{\pi^2 \hbar} \ln \left[\frac{L}{L_0} \right], \quad (2)$$

where α is a constant or order unity and is a measure of the amount of intervalley scattering, and L is the system's linear dimension. At $T=0$ and in a zero magnetic field, L would be given by the sample size, but at finite temperature T , or magnetic field B , L may be replaced by L_i (the inelastic diffusion length) or L_c [the cyclotron length $(\hbar/eB)^{1/2}$], or some combination of the two.

$\sigma(T)$ can be deduced from this via the temperature dependence of the inelastic scattering rate, τ_i , which can be approximately written as $\tau_i \propto T^{-p}$, where p is an index depending on the scattering mechanism, dimensionality, etc. This leads to

$$\sigma(T) = \sigma(T_0) + \frac{\alpha p e^2}{2\pi^2 \hbar} \ln \left[\frac{T}{T_0} \right]. \quad (3)$$

Following work by Alt'schuler, Aronhov, and Lee,⁸ Alt'schuler *et al.*,⁹ and Finkelstein,¹⁰ among others, it is

$$\begin{aligned} \sigma(T, B) = & \sigma(T_0, 0) + \frac{\alpha p}{2} \frac{e^2}{\pi^2 \hbar} \ln \left| \frac{T}{T_0} \right| + \frac{\alpha e^2}{2\pi^2 \hbar} \left[\psi(a + \frac{1}{2}) - \psi(a' + \frac{1}{2}) + 2 \ln \left| \frac{L_i}{l} \right| \right] \\ & + \frac{e^2}{4\pi^2 \hbar} (2 - \frac{3}{2} \bar{F}_\sigma) \ln \left| \frac{T}{T_0} \right| - \frac{\bar{F}_\sigma}{2} \frac{e^2}{2\pi^2 \hbar} g(h), \end{aligned} \quad (8)$$

where

$$a = \frac{\hbar}{2eBL_i^2}, \quad a' = \frac{\hbar}{2eBl^2}$$

expected that in the regime $k_F l \gg 1$, taking interactions into account, the conductivity will behave as

$$\sigma(T) = \sigma(T_0) + (2 - \frac{3}{2} \bar{F}_\sigma) \frac{e^2}{4\pi^2 \hbar} \ln \left[\frac{T}{T_0} \right], \quad (4)$$

where \bar{F}_σ is given by

$$\bar{F}_\sigma = \frac{8(1+F/2)\ln(1+F/2)}{F} - 4, \quad (5)$$

and F , which is a measure of the screening, is given by

$$F = \int_0^{2\pi} d\theta \frac{1}{2\pi} \frac{1}{1 + (2k_F/\kappa)\sin(\theta/2)}. \quad (6)$$

Here, κ is the inverse screening length in 2D,

$$\kappa = \frac{e^2 N(E_F)}{2\epsilon_0 \epsilon_r}. \quad (7)$$

Earlier theories included $(2-2F)$ in the prefactor of Eq. (4) rather than $2 - \frac{3}{2} \bar{F}_\sigma$, but these have since been revised. (See the review article by Lee and Ramakrishnan.¹¹)

As can be seen from (4) when $k_F/\kappa \rightarrow 0$, $F \rightarrow 1$, while when k_F/κ diverges $F \rightarrow 0$, so in a well-screened system there is very little temperature dependence due to electron-electron interactions. It is clear that (3) and (4) can be identical given appropriate values of α , p , and \bar{F}_σ ; consequently, a conductivity measurement cannot distinguish the dominant process involved. As can be seen from the form of (6) above, F should theoretically lie in the range $0 \leq F \leq 1$, implying \bar{F}_σ in the range⁸ $0 \leq \bar{F}_\sigma \leq 0.865$, with no possibility of values greater than unity.

Various workers have shown that the localization and interaction effects depend very differently on an applied magnetic field.¹¹ For perpendicular fields, 2D localization effects are reduced significantly when $L_c < L_i$, and as the localization phenomenon is an orbital effect in the plane of the 2D EG, it is unaffected by a parallel field. However, the major effect of the magnetic field on the interaction term is to introduce spin splitting of the energies of the up- and down-spin electrons, thus altering the effective density of states and the Fermi energy: this effect is largely independent of field orientation.

By taking all these features into account, the conductivity in two dimensions can be written as

and ψ is the digamma function. For a derivation of the term in ψ , see Hikami, Larkin, and Nagaoka.¹² h is the ratio of the spin-splitting energy to the thermal energy $h = g_L \mu_B B / k_B T$. The size of the interaction magneto-

conductivity is determined in terms of h by

$$g(h) = \int_0^\infty d\omega \left[\frac{d^2}{d\omega^2} \left(\frac{\omega}{e^\omega - 1} \right) \ln \left| 1 - \frac{h^2}{\omega^2} \right| \right]. \quad (9)$$

The different contributions to σ in (8) are difficult to untangle, but for the case of a constant-temperature, parallel-magnetic-field measurement the magnetoconductivity reduces to

$$\sigma(B_{\parallel}) = \sigma(0) - \frac{\tilde{F}_\sigma}{2} \frac{e^2}{2\pi^2\hbar} g(h), \quad (10)$$

and so fitting experimental data to the function $g(h)$ should enable the prefactor \tilde{F}_σ to be determined.

Lee and Ramakrishnan¹³ calculate the two limiting forms of $g(h)$ as

$$g(h) = 0.084h^2, \quad h \ll 1 \quad (11a)$$

$$g(h) = \ln \left| \frac{h}{1.3} \right|, \quad h \gg 1. \quad (11b)$$

Kawabata¹⁴ also derived limiting expressions for the conductivity based on similar arguments. We have evaluated (9) for all values of h (Ref. 13) (see the Appendix), and our result for $g(h)$ is shown in Fig. 1. The limiting forms of Kawabata's expression are also given in the Appendix, and the numerical coefficients quoted agree with those obtained from our evaluation to a high degree of accuracy.

Previous workers¹ have fitted parallel-field magnetoconductivity data to the limiting forms of $g(h)$ [(11a) and (11b)] and obtained values for F which exceed unity. They state that fitting the low-temperature $R(H)$ data to $\ln(h)$ and the high-temperature $R(H)$ data to h^2 "yields a similar value for F implying no strong temperature dependence to this parameter." By extending this procedure to include fitting to the whole function $g(h)$, as well as its limiting forms, we reveal a temperature dependence of \tilde{F}_σ . What is also evident from our fitting pro-

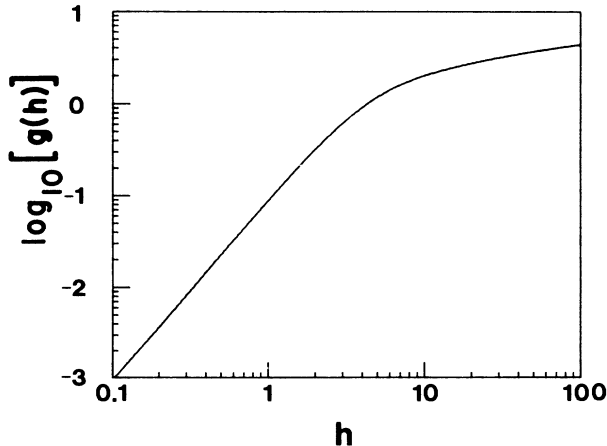


FIG. 1. The function $g(h)$ obtained by numerically integrating (9), showing the low- h parabolic regime and the high- h logarithmic regime.

cedure is that the theory function fits less well at lower temperatures, indicating either the perturbation-limit breakdown (i.e., $k_F l \sim 1$), or showing that the theoretical function $g(h)$ does not describe the experimentally observable behavior at very low temperatures.

Further useful information may be obtained by looking at the $B=0$ temperature dependence of conductivity,

$$\sigma(T) = \sigma(T_0) + \frac{\alpha p}{2} \frac{e^2}{\pi^2\hbar} \ln \left[\frac{T}{T_0} \right] + (2 - \frac{3}{2}\tilde{F}_\sigma) \frac{e^2}{4\pi^2\hbar} \ln \left[\frac{T}{T_0} \right]. \quad (12)$$

The factor $\alpha p + (1 - \frac{3}{4}\tilde{F}_\sigma)$ can then be extracted experimentally as a function of carrier concentration (or gate voltage). Given that αp has been uniquely determined from low-field perpendicular magnetoconductivity measurements, then \tilde{F}_σ can, in theory, be found unambiguously from the $\sigma(T)$ measurements.

Furthermore, if the temperature dependence of conductivity is measured with the sample placed in perpendicular magnetic field strong enough to reduce localization effects significantly, but not so strong that the interaction effects become important, the resulting temperature dependence should be given by the fourth term in (8) alone.

III. EXPERIMENTAL PROCEDURE

The devices studied were silicon MOSFET's fabricated on 14–20- Ω cm (100) p -type silicon with a gate oxide thickness of 1000 \AA , source to drain length of 300 μm , width 30 μm , and with voltage probes on both sides, one-third and two-thirds of the way along.

The cryostat used was a "single-shot," continuously pumped ^3He system, with a 300-mK base temperature and 10-T magnet.

The conductance of the inversion layer was measured using a true four-terminal technique. The measurement was made at approximately 79 Hz using a phase-sensitive detector. All measuring signals were kept low enough to prevent significant electron heating by the electric field across the sample (in practice, $< 1 \text{ V m}^{-1}$ in all cases).

Particular attention was paid to radio-frequency (rf) screening and filtering of the signal lines, to prevent coupling of rf into the sample, which would cause heating of the electron gas. All earth loops in the coaxial cable shields were prevented by using a "star" earthing arrangement, where the cryostat itself was only earthed via a single low-impedance connection to the electronics ground.

Very careful alignment of the sample is essential in a parallel-field measurement because the perpendicular effects become significant at magnetic fields at least an order of magnitude smaller than for the parallel effect. In principle, the Hall effect can be used to align the sample so that the magnetic field is accurately in the plane of the 2D EG. The Hall voltage depends only on the perpendicular component of the field: in a real sample it is necessary to look at the Hall resistance for both signs of magnetic field, to allow for any minor misalignment of the

voltage probes. By use of a top-loading cryostat, allowing sample adjustment through a small angle and reinsertion, we have been able to reduce field misalignment to $0.07^\circ \pm 0.01^\circ$, giving a perpendicular-field component of less than 7 mT when the total field is 5 T, which is necessary for these measurements.

A calibrated germanium resistance thermometer was mounted on the same copper tailpiece as the sample. Both devices had their wires firmly heat sunk to the copper, to ensure they were in thermal equilibrium.

IV. EXPERIMENTAL RESULTS

Our experimental measurements can be divided into four separate areas.

A. Parallel-field magnetoconductivity [$\sigma(B_{\parallel})$]

$\sigma(B_{\parallel})$ has been measured over the range $0 \leq B \leq 5$ T, and for various values of gate voltage (i.e., different values of $k_F l$), at temperatures of 4.2, 1.4, and 0.5 K. Figure 2 shows typical data at $V_g = 2.0$ V for these temperatures. The solid lines are generated by first numerically integrating $g(h)$ in (9) and then fitting (10) to the experimental data. Note that the fit becomes progressively worse as the temperature is lowered, indicating that the high- h behavior of $g(h)$ is incorrect. Because of this, the values of $\bar{F}_\sigma(T, V_g)$ shown in Fig. 3 are obtained by fitting the low- h parabolic limit of $g(h)$ to the 4.2-K data and the high- h logarithmic limit of $g(h)$ to the 0.5- and 1.4-K data. (Note that the values of F_σ obtained using the low- h parabolic limit at 4.2 K agree with those obtained from the full fitting procedure to within experimental uncertainty.) Also the values of \bar{F}_σ obtained from fitting the high- h limit of $g(h)$ at 1.4 K are consistently 82% of the value obtained from fitting the whole of $g(h)$. All this information points to the high- h limit of $g(h)$ being incorrect. It is also quite clear from Fig. 3 that \bar{F}_σ is temperature dependent, and can take values greater than the currently expected theoretical maximum of 0.865, which we have calculated from an expression given by Alt'shuler, Aronhov, and Lee.⁸

Figure 3 shows that F_σ behaves similarly versus V_g for all the temperatures studied, i.e., as $V_g \rightarrow 0$, \bar{F}_σ falls rapidly towards zero, while at higher values of V_g , \bar{F}_σ falls off gradually with increasing V_g . The gradual drop in \bar{F}_σ at high V_g has been seen previously in low-mobility, [111]-oriented samples,¹ but the rapid fall at very low V_g in our higher-mobility, [100]-oriented devices has not been reported before.

B. Low-field perpendicular magnetoconductivity

These data have been fitted to the digamma-function¹² expansion of (8), which allows extraction of τ_i and α . These parameters can be determined independently by this fitting method only if the magnetoconductivity shows a logarithmic regime, and this happens only at sufficiently

high gate voltage (V_g) or low temperature (T). For our data that show this logarithmic behavior, we find $\alpha = 0.5 \pm 0.1$, and so we have taken $\alpha = 0.5$ for all other values of V_g and T . τ_i ranges from 3 to 40 ps, depending on the temperature and gate voltage. Writing $\tau_i \propto T^{-p}$, we arrive at a value for $p = 1.02 \pm 0.22$ over a range of V_g , and so $\alpha p = 0.5$.

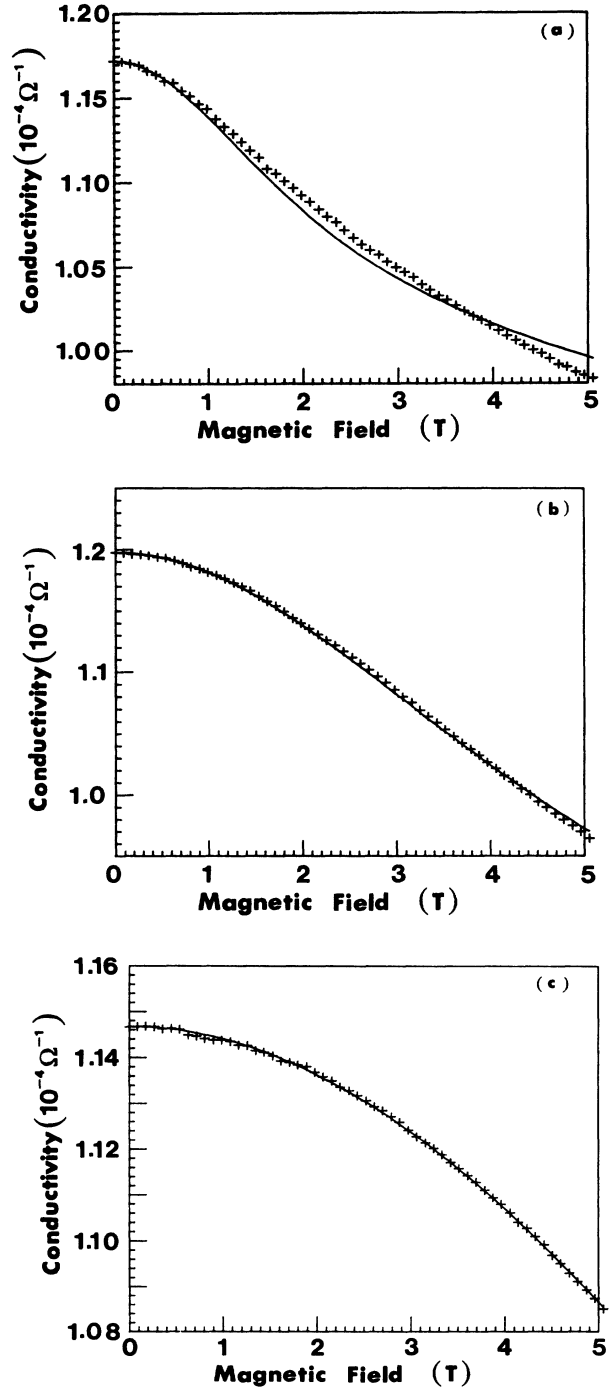


FIG. 2. Typical conductivity data at $V_g = 2$ V of the 2D EG formed under the gate of a Si MOSFET for (a) 0.5 K, (b) 1.4 K, and (c) 4.2 K. The solid line is generated by fitting $g(h)$ to the experimental data in each case.

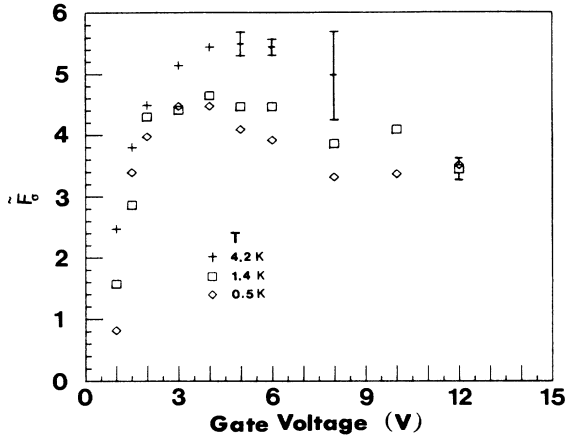


FIG. 3. \tilde{F}_σ extracted from fitting the limiting forms of $g(h)$ to the experimental data obtained from $\sigma(B_{\parallel})$ measurements as a function of gate voltage (hence E_F) for the three different temperatures studied.

C. Temperature dependence of conductivity at $B=0$

These data are shown plotted versus $\ln(T)$ at one particular value of gate voltage in Fig. 4. The gradient of σ versus $\ln(T)$ is given by (12) as a constant times $\alpha p + (1 - \frac{3}{4}\tilde{F}_\sigma)$. However, $\partial(\delta\sigma)/\partial(\ln T)$ is not a straight line, but deviates from logarithmic behavior at both ends. The low- T deviation occurs because if σ is to go to zero at $T=0$, then it cannot fall logarithmically indefinitely. At higher T , phonon scattering will tend to lower the conductivity. $\partial(\delta\sigma)/\partial(\ln T)$ is the gradient between these two regimes, and is shown plotted for several different gate voltages in Fig. 5.

$\partial(\delta\sigma)/\partial(\ln T)$ obtained via this method is an average gradient between $T=0.5$ and 0.9 K approximately, and so within the limitations of this analysis, we can assign an approximate temperature of 0.7 ± 0.2 K to this measurement. It must be pointed out that if \tilde{F}_σ is a strong func-

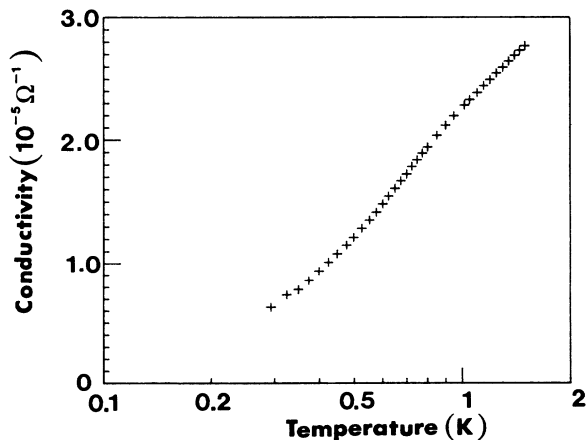


FIG. 4. Typical temperature dependence of conductivity $[\sigma(T)]$ at $V_g = 2$ V, showing the logarithmic dependence.

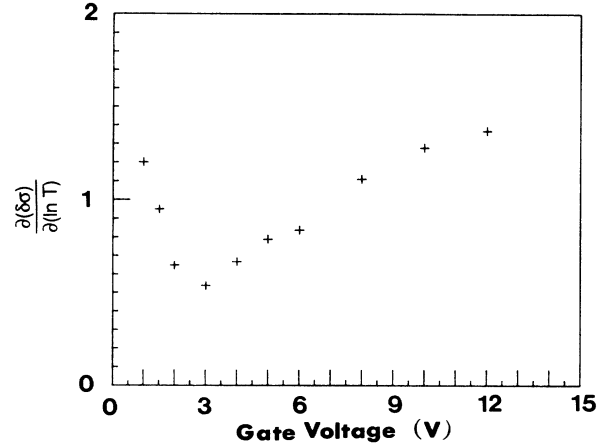


FIG. 5. The slope $\partial(\delta\sigma)/\partial(\ln T)$ extracted as a function of gate voltage.

tion of temperature, then the gradient $\partial(\delta\sigma)/\partial(\ln T)$ is not given by $\alpha p + (1 - \frac{3}{4}\tilde{F}_\sigma)$. Instead, an extra term in $\partial(\delta\sigma)/\partial(\ln T)$ is introduced. It may be for this reason that \tilde{F}_σ given by this method is slightly lower than would be expected from parallel-field magnetoconductivity measurements; however, as the exact form of $\tilde{F}_\sigma(T)$ is not known, it is not possible to proceed further with this analysis.

Given $\alpha p = 0.5$, \tilde{F}_σ can be determined independently of the parallel-magnetic-field measurements. The results of such a determination are shown in Fig. 6. Note that the qualitative behavior of \tilde{F}_σ versus V_g is reproduced, although the magnitude of \tilde{F}_σ is slightly lower than that obtained by parallel-field measurements.

D. Temperature dependence at $B_{\perp} = 0.1$ T

In this experiment we can effectively “turn off” the localization effects by ensuring that the cyclotron length L_c

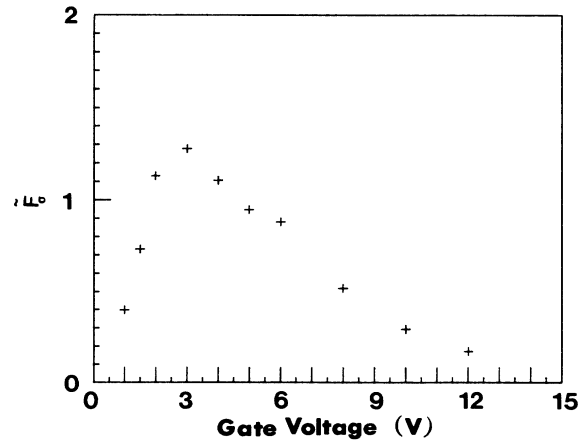


FIG. 6. \tilde{F}_σ derived from the gradients of the temperature dependence of conductivity as a function of gate voltage. (Note the qualitative similarity to Fig. 3.)

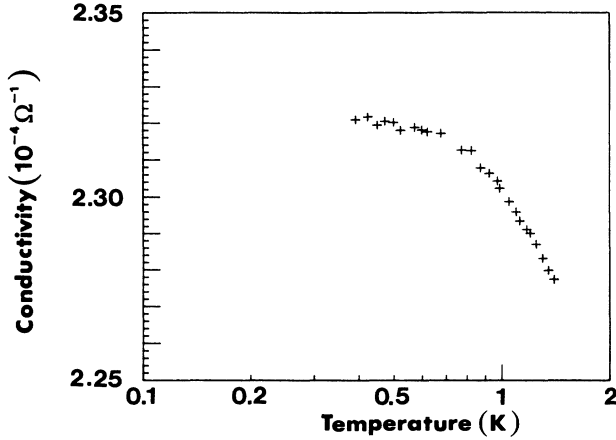


FIG. 7. $\sigma(T)$ with a small magnetic field applied perpendicular to the 2D EG at approximately 0.7 K. Note the negative gradient indicating $\bar{F}_\sigma > 1$.

is smaller than the inelastic scattering length L_i . [Care has to be taken to ensure that the magnetic field does not become so large that the magnetic energy $g\mu_B B$ approaches $k_B T$; otherwise, interaction effects will become significant, through the $g(h)$ term in (8).] This should leave the gradient of σ versus $\ln(T)$ as a constant multiplied by $1 - \frac{3}{4}\bar{F}_\sigma$. The gradient $\partial(\delta\sigma)/\partial(\ln T)$ is not constant as T varies (Fig. 7) and can be negative. By analyzing the variation of gradients, we have yet another way of extracting $\bar{F}_\sigma(V_g, T)$. Figure 8 shows $\bar{F}_\sigma(V_g)$ at $T = 300$ mK and 1.2 K. This method of determining \bar{F}_σ is again completely independent of the parallel-field magnetoconductivity measurements. The behavior is once more qualitatively the same as Fig. 3, i.e., as $k_F l$ is reduced to zero, \bar{F}_σ goes to zero, and \bar{F}_σ decreases as $k_F l$ is increased at higher values of $k_F l$. We also see a similar temperature dependence for \bar{F}_σ , i.e., an increase in \bar{F}_σ as T is increased.

For a magnetic field of 0.1 T, the cyclotron length is 80 nm. We have determined inelastic scattering lengths which are smaller than this for low gate voltages and high temperatures, so care is required in interpreting the results.

V. DISCUSSION OF RESULTS

The trends in the $\bar{F}_\sigma(V_g)$ curve (Fig. 3) can be tentatively explained as follows: \bar{F}_σ is given by (5) and (6) and is seen to be a function of k_F/κ , the ratio of the Fermi wave vector to the inverse static screening length. Because the density of states in two dimensions is normally considered to be constant, then from (7) κ is also constant. The Fermi wave vector is given by

$$k_F = \left(\frac{2E_F m^*}{\hbar} \right)^{1/2} \quad (13)$$

and E_F is proportional to V_g , so for large values of gate voltage, \bar{F}_σ would be expected to fall off as k_F is in-

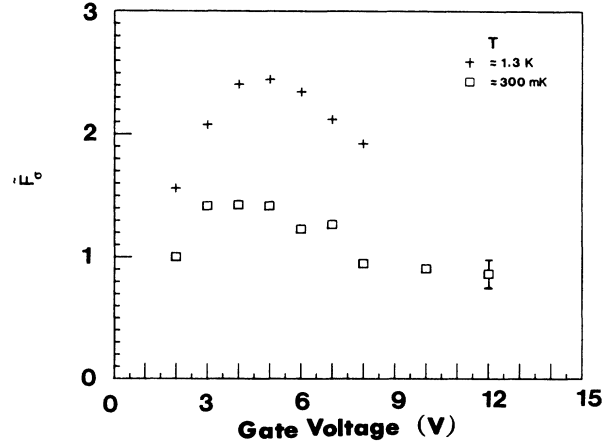


FIG. 8. \bar{F}_σ derived from the analysis of the gradients of the temperature dependence of conductivity with a small perpendicular magnetic field.

creased, which is in fact what is seen (as also observed by Bishop, Dynes, and Tsui¹).

The fall off of \bar{F}_σ as the gate voltage is reduced towards zero may be explained by the density of states $N(E_F)$ falling off faster than k_F as the bottom of the band is approached. This is not an unreasonable assumption because it is known that the density of states in the band tail ultimately falls off exponentially.¹⁵

Our experiments clearly and unambiguously show that the interaction parameter \bar{F}_σ varies with T . This temperature dependence is unexpected: theoretical work^{13,14} gives an \bar{F}_σ which is independent of T . A temperature dependence may indicate a contribution from inelastic processes that prior theoretical calculations have not included. At the lowest temperatures, inelastic effects should have the least impact, and any discrepancies due to these should be smallest. As pointed out earlier, calculations of F have all given values in the range 0–1, implying \bar{F}_σ in the range 0–0.865, with no possibility of values greater than 1. At most, T and V_g we get $\bar{F}_\sigma > 1$, but at the lowest T we obtain values for \bar{F}_σ of approximately 1.

Bishop, Dynes, and Tsui¹ did not report any variation of F with T . This may be due to the different substrate orientation, or the inadequacy of their fitting procedure for $g(h)$: they fitted only the logarithmic limit in the low- T (100 mK) regime and the parabolic limit in the high- T (4.2 K) regime, for their parallel-field data.

VI. CONCLUSIONS

In this work we have experimentally determined the dependence of \bar{F}_σ against carrier concentration (V_g) using three independent methods and find these results to be qualitatively consistent. They show \bar{F}_σ is larger than theoretically predicted at intermediate V_g , falling slowly at higher k_F and, previously unseen, dropping rapidly at low V_g . Furthermore, we have demonstrated a previously unreported temperature dependence in \bar{F}_σ .

Our results clearly point to the need for further theoretical work to explain how \tilde{F}_σ can vary with temperature and to qualitatively account for the dependencies of \tilde{F}_σ on carrier concentration. Experimentally it would be interesting to see the measurements extended to lower temperatures, where any discrepancies between experiment and current theory resulting from inelastic processes might be expected to be reduced.

ACKNOWLEDGMENTS

This work was funded by a United Kingdom Science and Engineering Research Council (SERC) award. One of us (M.S.B.) would like to acknowledge the financial support of the SERC. We would like to thank Alan Gundlach of the Edinburgh University Microfabrication Unit, who fabricated the devices used in this work, and John Inkson for many helpful discussions.

APPENDIX: EVALUATING $g(h)$

The function $g(h)$ which gives the form of the interaction magnetoconductivity has been determined in integral form^{11,13}

$$g(h) = \int_0^\infty d\omega \left[\frac{d^2}{d\omega^2} \left[\frac{\omega}{e^\omega - 1} \right] \ln \left| 1 - \frac{h^2}{\omega^2} \right| \right], \quad (\text{A1})$$

and these authors have calculated the limiting forms for small and large h to be

$$g(h) = 0.084h^2, \quad h \ll 1 \quad (\text{A2a})$$

$$g(h) = \ln \left| \frac{h}{1.3} \right|, \quad h \gg 1. \quad (\text{A2b})$$

Independently, Kawabata¹⁴ derived a series expression for g in terms of $b = h/2\pi$, with limiting forms that are, in terms of h ,

$$g(h) = 0.091h^2, \quad h \ll 1 \quad (\text{A3a})$$

$$g(h) = \ln \left| \frac{h}{1.29} \right| - \frac{\pi^2}{3h^2}, \quad h \gg 1. \quad (\text{A3b})$$

These two sets of results are very similar. Previous tests of experimental data have only involved fits to the high- and low- h limits, but it is important to be able to compare experiments with a more general expression for $g(h)$, especially at temperatures and magnetic fields for which h is of order unity.

We have evaluated expression (A1) by firstly rewriting it as

$$g(h) = \int_0^\infty dx \frac{(2+x)\ln(1+x) - 2x}{x^3} \ln \left| 1 - \frac{h^2}{[\ln(1+x)]^2} \right| \quad (\text{A4})$$

and integrating numerically. We confirm the above limiting values, obtaining

$$g(h) \rightarrow (0.091 \pm 0.001)h^2 \quad \text{as } h \rightarrow 0 \quad (\text{A5})$$

$$g(h) \rightarrow (1.000 \pm 0.0001) \ln[h/(1.298 \pm 0.001)] \quad \text{as } h \rightarrow \infty. \quad (\text{A6})$$

Furthermore, we find that numerically the size of the first order deviation from logarithmic behavior in the integral agrees to within 5% with Kawabata's expression (A3b). Figure 1 shows our computed $g(h)$ for $0.1 \leq h \leq 100$. Outside this range, (A5) and (A6) are accurate to 1% or better.

¹D. J. Bishop, R. C. Dynes, and D. C. Tsui, Phys. Rev. B **26**, 773 (1982).

²T. Ando, A. B. Fowler, and F. Stern, Rev. Mod. Phys. **54**, 437 (1982).

³D. J. Thouless, Phys. Rev. Lett. **39**, 1167 (1977).

⁴E. Abrahams, P. W. Anderson, D. C. Licciardello, and T. V. Ramakrishnan, Phys. Rev. Lett. **42**, 673 (1979).

⁵A. F. Efros and B. I. Shklovskii, J. Phys. C **8**, L49 (1975).

⁶B. L. Alt'shuler and A. G. Aronhov, Solid State Commun. **39**, 115 (1979a).

⁷B. L. Alt'shuler and A. G. Aronhov, Zh. Eksp. Teor. Fiz. **77**, 2028 (1979) [Sov. Phys.—JETP **50**, 968 (1979b)].

⁸B. L. Alt'shuler, A. G. Aronhov, and P. A. Lee, Phys. Rev. Lett. **44**, 1288 (1980).

⁹B. L. Alt'shuler, D. Khmel'nitskii, A. I. Larkin, and P. A. Lee, Phys. Rev. B **22**, 5142 (1980).

¹⁰A. M. Finkelstein, Zh. Eksp. Teor. Fiz. **84**, 168 (1983) [Sov. Phys.—JETP **57**, 97 (1983)].

¹¹P. A. Lee and T. V. Ramakrishnan, Rev. Mod. Phys. **57**, 287 (1985).

¹²S. Hikami, A. I. Larkin, and Y. Nagaoka, Prog. Theor. Phys. **63**, 707 (1980).

¹³P. A. Lee and T. V. Ramakrishnan, Phys. Rev. B **26**, 4009 (1982).

¹⁴A. Kawabata, Surf. Sci. **113**, 527 (1982).

¹⁵I. M. Lifshitz, Zh. Eksp. Teor. Fiz. **53**, 743 (1967) [Sov. Phys.—JETP **26**, 462 (1968)].